# Effect of mobile ions on the electric field needed to orient charged diblock copolymer thin films

Ashkan Dehghan, M. Schick, and An-Chang Shi

Citation: The Journal of Chemical Physics **143**, 134902 (2015); doi: 10.1063/1.4931826
View online: http://dx.doi.org/10.1063/1.4931826
View Table of Contents: http://scitation.aip.org/content/aip/journal/jcp/143/13?ver=pdfcov
Published by the AIP Publishing

# Effect of mobile ions on the electric field needed to orient charged diblock copolymer thin films

Ashkan Dehghan,[1] M. Schick,[2] and An-Chang Shi[1]
[1]*Department of Physics and Astronomy, McMaster University, Hamilton, Ontario L8S 4M1, Canada*
[2]*Department of Physics, University of Washington, Seattle, Washington 98195, USA*

(Received 11 June 2015; accepted 15 September 2015; published online 5 October 2015)

We examine the behavior of lamellar phases of charged/neutral diblock copolymer thin films containing mobile ions in the presence of an external electric field. We employ self-consistent field theory and focus on the aligning effect of the electric field on the lamellae. Of particular interest are the effects of the mobile ions on the critical field, the value required to reorient the lamellae from the parallel configuration favored by the surface interaction to the perpendicular orientation favored by the field. We find that the critical field depends strongly on whether the neutral or charged species is favored by the substrates. In the case in which the neutral species is favored, the addition of charges decreases the critical electric field significantly. The effect is greater when the mobile ions are confined to the charged lamellae. In contrast, when the charged species is favored by the substrate, the addition of mobile ions stabilizes the parallel configuration and thus results in an increase in the critical electric field. The presence of ions in the system introduces a new mixed phase in addition to those reported previously. © *2015 AIP Publishing LLC.* [http://dx.doi.org/10.1063/1.4931826]

## I. INTRODUCTION

Block copolymers are commonly utilized because of their ability to form self-assembled structures with wavelengths that scale as the size of the polymers. This is generally on the order of 10-100 nm. Such a property offers the possibility of many applications such as nanolithographic templates, nanostructured networks, stimuli-responsive materials, and well-ordered arrays of metal nanowires.[1,2] The challenge encountered when using thin films of block copolymers is that the creation of highly ordered, long-range, single-domain structures is often made difficult by interactions at the surface of the polymer film. These interactions often result in the formation of microdomains self-assembled parallel to the air or substrate interfaces. In many applications, however, the perpendicular orientation is the desired one. This problem has motivated the implementation of techniques for directing the self-assembly of block copolymers or for realigning the morphologies from the parallel to the perpendicular orientation.

A number of methods have been developed for directing the self-assembly of block copolymers and have been reviewed recently.[3] Among them are the use of pre-patterned substrates,[4–7] topographically modified substrates,[8–10] and external stimuli such as an electric field.[11–16] The electric field brings about alignment due to a difference in the dielectric constant of the different blocks of the polymers. The effects of the strength of this field, of the polymer-substrate interactions, and of the film thickness have been the subject of several experiments.[17–20] For example, Xu *et al.* investigated the effects of an external electric field on the cylinder forming diblock copolymers in thin films.[21] They showed that redirecting the formation of cylinders from the parallel configuration, caused by the selective polymer/substrate interaction, to the perpendicular orientation was made possible by application of the field.[21] In a theoretical study, Tsori and Andelman examined the alignment of microdomains formed by symmetric polystyrene-b-poly(methyl methacrylate) (PS-b-PMMA) in the presence of an external electric field as a function of film thickness and polymer/surface interactions.[13] They noted that the ability of the electric field to induce the self-assembly of microdomains in the direction parallel to it depends strongly on the film thickness. For some systems, the electric field required to reorient the morphologies might well result in the dielectric breakdown of the material.

To induce the formation of perpendicularly oriented microdomains in thin films by means of smaller electric fields, Tsori *et al.* suggested adding mobile ions.[22,23] The reasoning is that the electrostatic potential energy of a dipole moment per unit volume, $\mathbf{P}$, in an electric field, $\mathbf{E}$, is $-\mathbf{P}\cdot\mathbf{E}$. The battery keeps the total electric field across the film constant. Because the dipole moment depends upon the separation of charges, the addition of mobile charges is expected to increase this separation and thereby increase the difference in the energy of the parallel and perpendicular orientations. The unstated assumption is that the increase in dipole moment is larger in the perpendicular orientation than in the parallel one. They also suggested that Li ions, present in the system from the anionic polymerization process, might be responsible for the success in bringing about reorientation of the microdomains. Any significant role that ions play can easily be discerned by applying an orienting, frequency-dependent, electric field. At low frequencies, the effect of free ions would be manifest and would vanish at higher frequencies. It was noted[24] that there was no frequency dependence in some successfully oriented films of PS-PMMA.[25] Nonetheless, when lithium chloride was

 

intentionally added io the system, the effect due to the free ions was quite clear.[25] Equally clear was the effect of doping a PS-PMMA system with lithium triflate, a salt which dissolves almost completely in the PMMA and much less so in the PS.[26]

The reasons for the success of free ions in reducing the value of the electric field needed to reorient the self-assembled domains and the generality of the result is less clear. Wang *et al.* attribute the success to a complexation of Li ions with carbonyl groups in the PMMA which enhances the difference between the dielectric constants of the PMMA and PS blocks.[25] In contrast, Kohn *et al.* take an approach[26] more in the spirit of the original suggestion of Tsori *et al.* in that they treat their system as a simplified one, consisting of alternating dielectric and conducting slabs. They calculate the torque on the interfaces due to the mobile ions. In a similar spirit, Putzel *et al.* considered a toy model consisting of alternating layers of two materials, A and B, characterized by different dielectric constants.[14] The A layers were uniformly charged, with mobile counter ions providing charge neutrality. The substrate preferred the B layers. They investigated the effect of selectively localizing the counter ions within one of the two blocks. They found that if the counter ions were confined such that *each* layer of A material was electrically neutral, then the value of the electric field needed to bring about a perpendicular orientation was indeed decreased by the addition of ions. This was attributed to the fact that only in the perpendicular configuration could an extensive polarization be brought about, i.e., an induced dipole moment per unit volume with a charge separation on the order of the film thickness. However, if the counter ions were free to migrate so that the system as a whole was electrically neutral but that individual layers of A were not, then the addition of charges did not necessarily decrease the field needed to reorient the system. Indeed they found that if the substrate preferred the A layers, then addition of ions could well *increase* the field needed for reorientation.

In this paper, we consider a system of lamellar forming AB diblock copolymers. The A polymers are partially charged and the system contains mobile counter ions which provide charge neutrality (Figure 1). Similar systems have been considered previously,[27–31] although their objective was to determine the effect of the charges on the phase diagram of the polymeric systems, not the effect of an external electric field on one of the microphases, as is the case here. In our study, the free energy of the system is obtained by employing self-consistent field theory (SCFT), as in several of the previous calculations.[28,30,31] As a consequence, the location of all charges is determined by a Poisson-Boltzmann equation. We also consider the effects of localization of charge within one block or the other and of the preference of the substrate for the blocks. We find for the case in which the substrate prefers the uncharged B polymers, as in the PMMA-PS system in which the PS is preferentially adsorbed,[32] the critical field needed to reorient the system decreases markedly even with the small concentration of ions utilized in experiment, typically parts in $10^{-3}$. Were the substrate to prefer the charged polymer, however, we find that the addition of free ions increases the field needed to reorient the system, in agreement with Putzel *et al.*[14] Such a prediction could be easily tested.

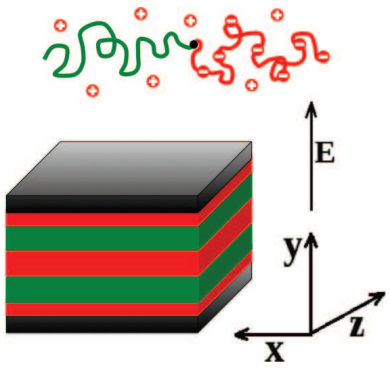


FIG. 1. A schematic diagram showing the model system examined in this work.

## II. THEORETICAL MODEL

We consider a system in volume $\Omega$ of $n_{AB}$ AB diblock copolymers with negatively charged A blocks and neutral B blocks. The index of polymerization is $N_{AB}$, so that the monomer density is $\rho_0 = n_{AB}N_{AB}/\Omega$. There are $n_I$ mobile positive counter ions with density $\rho_I = n_I/\Omega$. We define dimensionless densities for polymers and ions as

$$\hat{\Phi}_A(\mathbf{r}) = \frac{N_{AB}}{\rho_0}\sum_{i=1}^{n_{AB}}\int_0^f ds\ \delta(\mathbf{r}-\mathbf{R}_i^A(s)),$$
$$\hat{\Phi}_B(\mathbf{r}) = \frac{N_{AB}}{\rho_0}\sum_{i=1}^{n_{AB}}\int_f^1 ds\ \delta(\mathbf{r}-\mathbf{R}_i^B(s)), \qquad (2.1)$$
$$\hat{\Phi}_I(\mathbf{r}) = \frac{1}{\rho_I}\sum_{i=1}^{n_I}\delta(\mathbf{r}-\mathbf{r}_i^I),$$

where $f$ is the fraction of A in the AB diblock copolymer chain. In the above equation, $\mathbf{R}^A(s)$ and $\mathbf{R}^B(s)$ are space curves specifying the position of polymer segment $s$ along the chain. Similarly, $\mathbf{r}^I$ represents the position of the ions in the system. We assume that the free ions are positively charged and that there is a uniform negative charge density on the A blocks. The degree of ionization of the A block is $P_A$ and, as noted above, is quite small in experiment. Charge neutrality implies that the densities of ions and polymers is related by $\rho_I = P_A f\rho_0$. In our study, we ignore ion pairs.[29] The polymers are confined between plates separated by a distance $L$, with a potential difference $V_0$ between them, one which is maintained by a battery. The electrostatic energy of the system, which includes the battery, is a functional of the charge densities,

$$U[\hat{\Phi}_I,\hat{\Phi}_A] = -\frac{1}{2}\int d\mathbf{r}\ \epsilon(\mathbf{r})[\nabla V(\mathbf{r})]^2 + \rho_0 P_A f\int d\mathbf{r}\ eV(\mathbf{r})[\hat{\Phi}_I(\mathbf{r}) - \frac{\hat{\Phi}_A(\mathbf{r})}{f}], \qquad (2.2)$$

where $e$ is the unit of charge and $V(\mathbf{r})$ is the electric potential which itself is a functional of the charge densities via the Maxwell equation,

$$\nabla\cdot[\epsilon(\mathbf{r})\nabla V(\mathbf{r})] = -eP_A f\rho_0\left[\hat{\Phi}_I(\mathbf{r}) - \hat{\Phi}_A(\mathbf{r})/f\right]. \qquad (2.3)$$

The dielectric constant, $\epsilon(\mathbf{r})$, is position-dependent because the concentration of the two blocks varies in space. We

approximate the local dielectric constant by its volume-fraction weighted-average $\epsilon(\mathbf{r}) = \epsilon_0[\kappa_A\hat{\Phi}_A(\mathbf{r}) + \kappa_B\hat{\Phi}_B(\mathbf{r})]$. This approximation is clearly correct in the limits in which the volume fraction of one component approaches zero or unity. It captures the essential variation and has the advantage of simplicity, which is why it is commonly employed.[24,29] We assume that the dielectric constants are independent of the applied field and take $\kappa_A = 6.0$, appropriate for PMMA, and $\kappa_B = 2.5$ appropriate for PS.

In addition to the electrostatic energy, there is also the energy of interaction between the A and B monomers with strength given by a Flory parameter $\chi_{AB}$ and the surface interaction of the polymers with the plates, $h(\mathbf{r})$. Furthermore, to test the idea that increased confinement of the mobile charges should have a large effect on the critical value of the aligning field, we control the relative solubility of the mobile charges by introducing an *ad hoc* repulsive interaction between them and the B monomers, an interaction of a strength we denote $\chi_{BI}$.

The total energy functional is

$$\begin{aligned} H[\hat{\Phi}_A,\hat{\Phi}_B,\hat{\Phi}_I] &= U[\hat{\Phi}_I,\hat{\Phi}_A] + k_BT\rho_0\int d\mathbf{r}[\chi_{AB}\hat{\Phi}_A(\mathbf{r})\hat{\Phi}_B(\mathbf{r}) \\ &\quad + \chi_{BI}\hat{\Phi}_B(\mathbf{r})\hat{\Phi}_I(\mathbf{r})] \\ &\quad - k_BT\rho_0\int d\mathbf{r}\, h(\mathbf{r})[\hat{\Phi}_A(\mathbf{r}) - \hat{\Phi}_B(\mathbf{r})]. \end{aligned} \tag{2.4}$$

The thermodynamic properties of the system are conveniently described in the canonical ensemble, with fixed volume, temperature, and concentrations. The partition function is

$$\begin{aligned} Z = \frac{1}{\lambda_I^{3n_I}n_I!\lambda^{3n_{AB}}n_{AB}!}\Big[\int\prod_{i=1}^{n_{AB}} D[\mathbf{R}_i^{AB}(s)]P_{AB}[\mathbf{R}_i^{AB}(s)]\Big] \\ \times\Big[\int\prod_{i=1}^{n_I} d\mathbf{r}_i^I\Big]\int D[V(\mathbf{r})]\exp(-\beta H[\hat{\Phi}_A,\hat{\Phi}_B,\hat{\Phi}_I,V]) \\ \times\delta\Big(\hat{\Phi}_A(\mathbf{r}) + \hat{\Phi}_B(\mathbf{r}) - 1\Big), \end{aligned} \tag{2.5}$$

where $\beta \equiv 1/k_BT$, and $\lambda_{AB}$ and $\lambda_I$ are the thermal de Broglie wavelengths of the polymers and ions, respectively. We have assumed that the system is incompressible and have ignored the volume of the mobile ions. The polymers are treated as flexible Gaussian chains with configurations weighted by the Weiner measure,

$$P_{AB}[\mathbf{R}_i^{AB}(s)] \propto \exp\Big[-\frac{3}{2N_{AB}b_\circ^2}\int_0^1 ds\Big(\frac{d\mathbf{R}_i^{AB}(s)}{ds}\Big)^2\Big], \tag{2.6}$$

where $b_\circ$ is the Kuhn length of the polymers.

We obtain the free energy of this system within the SCFT approximation. There are excellent reviews of this approximation as it is applied to polymeric systems[33–35] and clear explications of its applications to systems with applied electric fields.[15,24,35] For completeness, we provide a brief derivation in the Appendix. As outlined there, within self-consistent field theory, $\beta F_{scft}/n_{AB}$, the free energy per polymer in units of $k_BT$, can be written as

$$\begin{aligned} \frac{\beta F_{scft}}{n_{AB}} &= -\ln\Big(\frac{Q_{AB}}{n_{AB}}\Big) - \frac{1}{\Omega}\int d\mathbf{r}\,\chi_{AB}N_{AB}\Phi_A(\mathbf{r})\Phi_B(\mathbf{r}) \\ &\quad + \frac{1}{\Omega}\int d\mathbf{r}\,[\beta eV(\mathbf{r})P_AN_{AB}f\Phi_I(\mathbf{r}) \\ &\quad + P_AN_{AB}f\Phi_I(\mathbf{r})\ln\Phi_I(\mathbf{r})]. \end{aligned} \tag{2.7}$$

Here, $\Phi_I(\mathbf{r})$ is the ensemble average value of $\hat{\Phi}_I(\mathbf{r})$, the dimensionless density of the counter ions, in the presence of an electric potential $V(\mathbf{r})$,

$$\Phi_I(\mathbf{r}) = \frac{\exp[-\beta eV(\mathbf{r})]}{(1/\Omega)\int d\mathbf{r}\exp[-\beta eV(\mathbf{r})]}, \tag{2.8}$$

so that the last two terms in the above free energy are simply the free energy of the counter ions. The first term in the free energy, $F_{scft}$, is the free energy per polymer in the single polymer ensemble. As the latter double-counts all binary interactions, it has to be corrected by the binary interactions of the second term. The functions $\Phi_A(\mathbf{r})$ and $\Phi_B(\mathbf{r})$ are the ensemble-average values of the local volume fractions $\hat{\Phi}_A(\mathbf{r})$ and $\hat{\Phi}_B(\mathbf{r})$ in the single polymer chain ensemble with partition function $Q_{AB}$ given below. Within self-consistent field theory, the potential is related via the Maxwell equation to the thermodynamic averages of the charge densities,

$$\nabla\cdot[\epsilon(\mathbf{r})\nabla V(\mathbf{r})] = -eP_Af\rho_0[\Phi_I(\mathbf{r}) - \Phi_A(\mathbf{r})/f], \tag{2.9}$$

and the local dielectric constant is now approximated by

$$\epsilon(\mathbf{r}) = \epsilon_0[\kappa_A\Phi_A(\mathbf{r}) + \kappa_B\Phi_B(\mathbf{r})]. \tag{2.10}$$

The partition function of the single polymer ensemble is obtained from the end-integrated propagator, $q(\mathbf{r},s)$, which satisfies the modified diffusion equation,

$$\frac{\partial q(\mathbf{r},s)}{\partial s} = [R_g^2\nabla^2 - iW_A(\mathbf{r})]q(\mathbf{r},s) \qquad 0 \le s \le f \tag{2.11}$$

$$= [R_g^2\nabla^2 - iW_B(\mathbf{r})]q(\mathbf{r},s) \qquad f < s \le 1, \tag{2.12}$$

where $R_g$ is the polymer's radius of gyration, and the fields are given by

$$\begin{aligned} \frac{iW_A(\mathbf{r})}{N_{AB}} &= \chi_{AB}\Phi_B(\mathbf{r}) - \frac{\kappa_A}{8\pi\rho_0\ell}[\nabla\beta eV(\mathbf{r})]^2 \\ &\quad - P_A\beta eV(\mathbf{r}) - h(\mathbf{r}) - i\frac{\xi(\mathbf{r})}{N_{AB}}, \end{aligned} \tag{2.13}$$

$$\begin{aligned} \frac{iW_B(\mathbf{r})}{N_{AB}} &= \chi_{AB}\Phi_A(\mathbf{r}) + \chi_{BI}\Phi_I(\mathbf{r}) - \frac{\kappa_B}{8\pi\rho_0\ell}[\nabla\beta eV(\mathbf{r})]^2 \\ &\quad + h(\mathbf{r}) - i\frac{\xi(\mathbf{r})}{N_{AB}}, \end{aligned} \tag{2.14}$$

where $\ell \equiv \beta e^2/4\pi\epsilon_0$ is the Bjerrum length. The propagator satisfies the initial condition $q(\mathbf{r},0) = 1$. It is also convenient to define the propagator, $q^\dagger(\mathbf{r},s)$, integrated from the other end of the polymer. It satisfies

$$\frac{\partial q^\dagger(\mathbf{r},s)}{\partial s} = -[R_g^2\nabla^2 - iW_A(\mathbf{r})]q^\dagger(\mathbf{r},s) \qquad 0 \le s \le f \tag{2.15}$$

$$= -[R_g^2\nabla^2 - iW_B(\mathbf{r})]q^\dagger(\mathbf{r},s) \qquad f < s \le 1, \tag{2.16}$$

with the boundary condition $q^\dagger(\mathbf{r},1) = 1$. The single polymer partition function is then obtained from

$$Q_{AB}[W_a,W_B] = \frac{1}{\lambda_{AB}^3}\int d\mathbf{r}\,q(\mathbf{r},1), \tag{2.17}$$

and the ensemble averages of the dimensionless monomer densities from

$$\Phi_A(\mathbf{r}) = \frac{\Omega}{\lambda_{AB}^3 Q_{AB}} \int_0^f ds\, q(\mathbf{r},s) q^\dagger(\mathbf{r},s), \qquad (2.18)$$

$$\Phi_B(\mathbf{r}) = \frac{\Omega}{\lambda_{AB}^3 Q_{AB}} \int_f^1 ds\, q(\mathbf{r},s) q^\dagger(\mathbf{r},s). \qquad (2.19)$$

The field $i\xi(\mathbf{r})$ in Eqs. (2.13) and (2.14) is a Lagrange multiplier adjusted so that the incompressibility condition

$$\Phi_A(\mathbf{r}) + \Phi_B(\mathbf{r}) = 1 \qquad (2.20)$$

is satisfied locally. Equations (2.8), (2.9), and (2.18) constitute the Poisson-Boltzmann equation.

The Maxwell equation (2.9) and five equations (2.13), (2.14), and (2.18)–(2.20) determine self-consistently the electrostatic potential, $V(\mathbf{r})$, and the five unknown fields $W_A(\mathbf{r})$, $W_B(\mathbf{r})$, $\Phi_A(\mathbf{r})$, $\Phi_B(\mathbf{r})$, and $\xi(\mathbf{r})$. They are solved in two dimensions using a combination of pseudo-spectral and finite-difference methods with appropriate initial and boundary conditions for a given phase.[36,37]

We fix the potential difference across the thin film by setting the value of electrostatic potential at the top and bottom surfaces to $V_{\mathbf{top}} = 0$ and $V_{\mathbf{bottom}} = V_0$. In addition, we keep the height of the film constant at $L = 2d_0$, where $d_0$ is the natural period of the lamellae for neutral AB diblock copolymers in bulk. We choose the height to be an integer value of $d_0$ as the parallel configuration is then most stable.[38,39] Therefore, the calculated value of the electric field needed to reorient the film will be an upper bound. We take the strength of interaction between the A and B species to be $\chi_{AB}N_{AB} = 20$. Finally, we must specify the interaction, $h(\mathbf{r})$, between the polymers and the substrate. The interactions are complex and their theoretical description is difficult, as noted by Messina *et al.* in their review.[40] However, our interest here is not in the origin of this attraction between substrate and polymer, but in the value of an imposed electric field needed to overcome the effect of this interaction which favors the parallel configuration. Hence, we approximate the interaction by the simple function $h(\mathbf{r})$ which takes the value $\mu$ at the plates and which is zero otherwise.

## III. RESULTS

In this section, we present our results on the phase behavior of the charged AB diblock copolymers as a function of electric field strength, charge density, and surface interactions. The blocks are lamellae forming with equal polymerization index so the volume fraction, $f$, of A monomer is 1/2. We consider two scenarios. In the first, the neutral B species interacts favorably with the top and bottom surfaces, which results in the aggregation of the B segments to a thickness of about $d_0/4$ at both substrate interfaces (Fig. 1). In the second, the charged A species interacts favorably with the top and bottom substrates.

We now consider the first scenario. In this case, the polymer/substrate interaction favors the parallel morphology with the B species aggregated at the top and bottom surfaces. One can bring about a phase transition from the parallel to the perpendicular phase by applying an external field perpendicular to the substrate. Figure 2 presents the free energy difference between the perpendicular and parallel morphologies as a function of dimensionless electric potential $\beta e\Delta V$ for neutral and charged systems. Here, we consider copolymers in which the fraction, $P_A$, of polymer which is ionized is small, $P_A = 0.0$, 0.001, and 0.002. This is comparable to experiment.[26,32] We note that for both neutral and charged thin films, the parallel phase has the lowest free energy at small values of $\Delta V$. An increase in the applied voltage results in a phase transition from the parallel to the perpendicular phase at some critical voltage $\Delta V_c$.

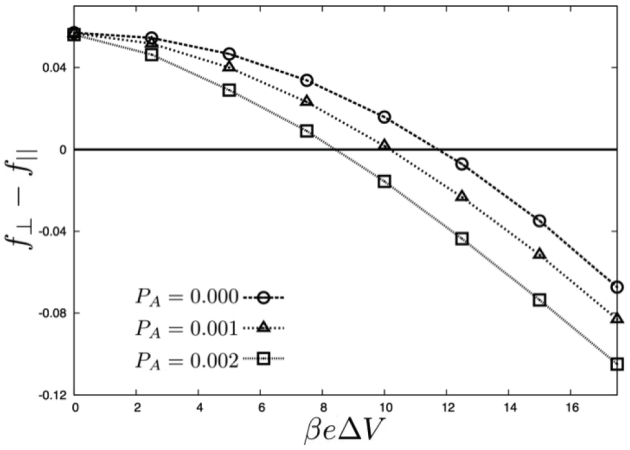


FIG. 2. Difference in the free energy between the perpendicular and the parallel phases as a function of applied voltage for copolymers characterized by $\chi_{AB}N_{AB} = 20$, $\chi_{BI}N_{AB} = 0$, $\kappa_A = 6.0$, $\kappa_B = 2.5$, and $\mu = -1$.

From Figure 2, we see that the addition of mobile charges does indeed lower the voltage required to orient the lamellae from the parallel to the perpendicular orientation. Furthermore, the reduction can be large, even for small amounts of added free charge. With the parameters chosen in the figure, addition of only two parts per thousand of mobile ions reduces the critical voltage by about 30%. This can be understood in terms of the polarization in the two orientations. In the case considered here, the positive counter ions are free to move throughout the system; however, the negative charges are bound to the A chains and thus are confined within the A domains. In the presence of an applied external field, charge separation in the perpendicular phase is of the order of the film thickness $L = 2d_0$, where $d_0$ is the period of the AB system in bulk. In the parallel orientation, however, the interposition of a layer of the neutral B polymers of thickness $d_0/4$ between the anode and the nearest lamella of negatively charged A polymers results in a separation of charge which is no greater than $L - d_0/4 = 7d_0/4$, significantly smaller than that in the perpendicular phase. Therefore, the addition of charge favors the perpendicular phase and lowers the voltage required to reorient the lamellae domains. Note however that the difference in charge separation in the two orientations, $d_0/4$, does not scale with the film thickness as the total free energy does. Hence as the thickness of the film increases, we expect the magnitude of the reduction in critical field due to the ions to decrease.

To further examine the effect of charge separation on the critical voltage, we consider a system in which the positive counter ions are increasingly confined to the A domains. We

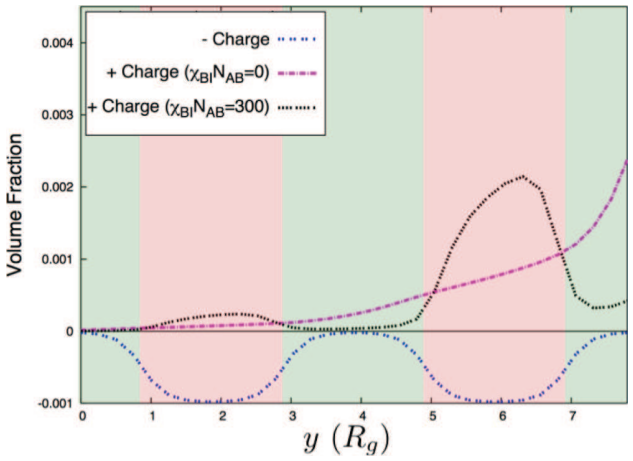


FIG. 3. One dimensional charge distribution for the charged AB system with $P_A = 0.001$, $\chi_{AB}N_{AB} = 20$, $\kappa_A = 6.0$, and $\kappa_B = 2.5$ with $\chi_{BI} = 0$ and $\chi_{BI} = 300$. The positive and negative electrodes are at $y = 0$ and $y = 8R_g$, respectively. The AB polymer distribution is shown as red/green shades, respectively, where in this case, B species are attracted by the substrates.

achieve this by introducing a repulsive interaction, $\chi_{BI}N_{AB}$, between the positive counter ions and the B monomers. As shown in Fig. 3, an increase in $\chi_{BI}N_{AB}$ results in a depletion of the positive ions from the domain near the negative electrode, thus resulting in a smaller separation of charge. The constraint of the confinement increases the free energy of both orientations at a rate proportional to the average overlap of ions and B monomers. It is not difficult to see that this overlap is large in the parallel configuration at the plate at which the ions tend to aggregate, a plate covered by B polymers. The free energy of this configuration, favored in the absence of an applied field, rapidly increases with ion confinement. The overlap is much lower in the perpendicular orientation; hence, the free energy advantage of the parallel phase rapidly decreases with the consequence that the critical voltage needed to bring about reorientation decreases.

The effect of confinement is evident from Fig. 4 which shows the critical voltage $\Delta V_c$ as a function of the fraction, $P_A$, of free ions for various values of the interaction parameter $\chi_{BI}N_{AB}$. As can be seen, the effect of the confinement of the ions is quite large. In terms of charge separation, we expect it to scale with the film thickness $L$ in the perpendicular configuration, but to be independent of $L$ in the confined, parallel configuration. Hence in this case, the difference in charge separation does scale with film thickness, and we expect the reduction in critical field due to the ions to persist as the film thickness increases.

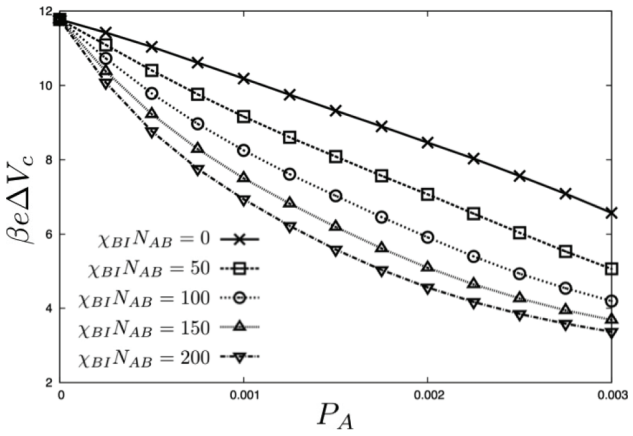


FIG. 4. The critical voltage $\Delta V_c$ plotted as a function of the degree of ionization $P_A$ for a system with $\chi_{AB}N_{AB} = 20$, $\kappa_A = 6.0$, $\kappa_B = 2.5$, and $\mu = -1$.

We now consider the effects of the strength of the surface interactions, $\mu$, on the voltage required to reorient the lamellae morphologies. Larger magnitudes of the negative surface field, $\mu$, correspond to a greater attractive interaction between the substrate and the B monomers relative to the A monomers. We begin with the simple case of neutral AB diblock copolymer thin films, subjected to an applied external voltage. Figure 5 presents the phase diagram of the neutral AB diblock copolymer thin films in the $\beta e\Delta V - \mu$ plane. Here, we consider three distinct phases: the parallel (Para), the perpendicular (Perp), and the mixed (Mix) phases. The mixed phase is composed of parallel and perpendicular morphologies (see Figure 6). For systems with $\mu = 0$, application of an infinitesimal electric field results in the instability of the parallel phase. As expected, a non-vanishing surface field stabilizes the parallel phase. The critical voltage required to reorient the lamellae from the parallel to the perpendicular phase increases as the strength of the surface interaction increases as expected. There exist a critical surface interaction $\mu_c$ beyond which an increase in the voltage results in a phase transition from the parallel to the mixed phase. In this region of the phase space, the surface interactions are strong enough to induce the formation of a thin partial wetting layer of B species at both surfaces. Away from the substrate, however, the electric field results in the formation of perpendicular domains. Because of this surface layer of B monomers, the cost of reorienting the lamellae to align with the field is not as great as in the simple perpendicular phase. Hence, the rate at which the critical field increases with surface field is less in going from the parallel configuration to the mixed phase than it is in going from the parallel phase to the simple perpendicular phase. This is an effect that cannot be captured by the toy models employed

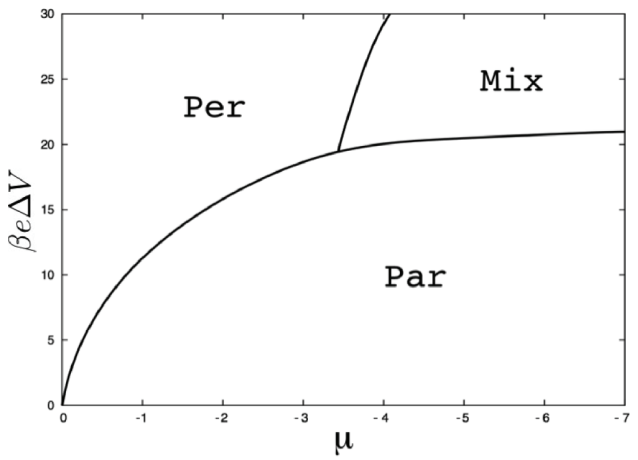


FIG. 5. Phase diagram for the neutral AB system with $P_A = 0$, $\chi_{AB}N_{AB} = 20$, $\chi_{BI}N_{AB} = 0$, $\kappa_A = 6.0$, and $\kappa_B = 2.5$ in the $\beta e\Delta V$-$\mu$ plane. The Per, Par, and Mix phases correspond to the perpendicular, parallel, and mixed phases, respectively.

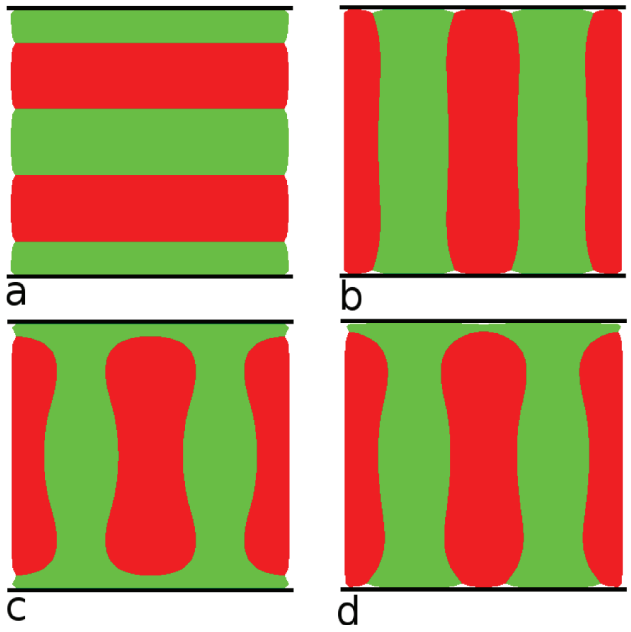


FIG. 6. Density profiles for the (a) parallel, (b) perpendicular, (c) mixed, and (d) partially mixed phases. Here, B species are green and A species are red. The top/bottom electrodes are negatively/positively charged.

previously.[14] Figures 6(a)–6(c) show the density profiles for the parallel, the perpendicular, and the mixed phases.

To the above uncharged system, we add a uniform negative charge distribution to the A blocks and positive counter ions. The effect on the phase diagram in the $\beta e\Delta V - \mu$ plane is shown in Figure 7 for a system with $P_A = 0.001$. As in the neutral system, at $\mu = 0$ the parallel phase becomes unstable when subjected to an infinitesimally small voltage. A non-zero $\mu$ stabilizes the parallel phase and results in an increase in the critical voltage. What is new in the charged system is the presence of a partially mixed phase (denoted P-Mix in Figure 7), which appears between the perpendicular and the mixed phases. To determine the difference between the two mixed phases, we examine their density profiles.

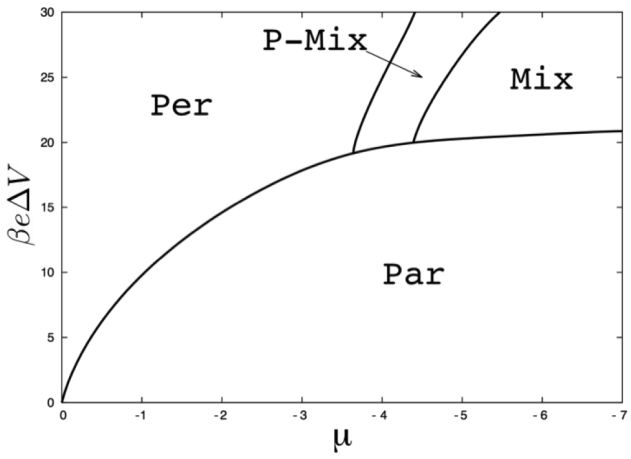


FIG. 7. Phase diagram for the charged AB system with $P_A = 0.001$, $\chi_{AB}N_{AB} = 20$, $\chi_{BI}N_{AB} = 0$, $\kappa_A = 6.0$, and $\kappa_B = 2.5$ in the $\Delta V$-$\mu$ plane. The Per, Par, Mix, and P-Mix phases correspond to the perpendicular, parallel, mixed, and partially mixed phases, respectively.

Figures 6(c) and 6(d) present the density profiles for the mixed and partially mixed phases, respectively. In the charged system, the parallel, perpendicular, and mixed phases are similar to those observed in the neutral system. The difference between the two mixed phases is seen as a difference in surface behavior. The electrostatic interaction between the negative A segments and the charged electrodes favors a partial wetting of the positively charged plate (bottom surface) by the A monomers, whereas the surface interaction, $\mu$, favors the partial wetting of *both* top and bottom surfaces by the B species. The presence of charge introduces an asymmetry which results in the formation of the partially mixed phase, Figure 6(d). For larger surface fields, the asymmetry is less important and the B species will partially wet both top and bottom surfaces, Figure 6(c).

We now consider the scenario in which the charged A species is attracted to the top and bottom surfaces. In this case, in the absence of an external electric field, the parallel phase with the A species partially wetting the polymer/substrate interface is the most stable structure. We begin by analyzing the phase transition between the parallel and perpendicular morphologies as a function of applied external voltage. Figure 8 presents the difference in the perpendicular and parallel free energies as a function of external voltage $\Delta V$ for neutral and charged thin films with $P_A = 0$, 0.001 and 0.002, respectively. As expected, for both neutral and charged copolymers, the parallel phase has the lowest free energy at small values of applied external voltage. Increase in $\Delta V$ results in a phase transition from the parallel to perpendicular phase at some critical $\Delta V_c$ value. In contrast to the previous case, in which the neutral B polymers were attracted to the surfaces, adding charge now *increases* the critical voltage required to reorient the lamellae from the parallel to the perpendicular orientation. An increase in $P_A$ further *stabilizes* the parallel phase. To examine this effect, we analyze the charge distribution within the system.

In the previous case with the neutral B species partially wetting the substrate interfaces, the charge separation in the parallel phase was smaller than the charge separation in the perpendicular phase, which resulted in a decrease in $\Delta V_c$ with

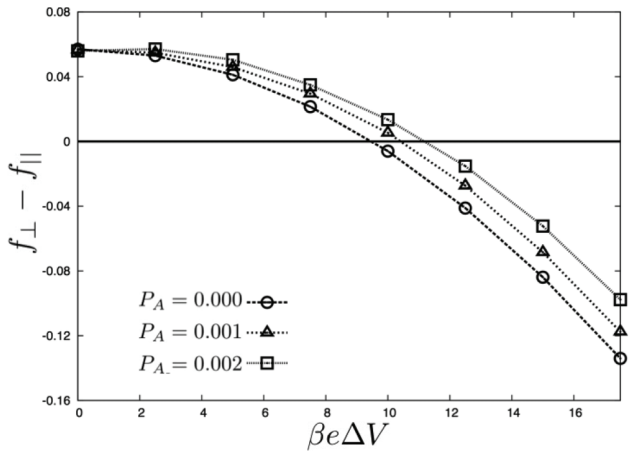


FIG. 8. Difference in the free energy between the perpendicular and the parallel phases for a system with $\chi_{AB}N_{AB} = 20$, $\chi_{BI}N_{AB} = 0$, $\kappa_A = 6.0$, $\kappa_B = 2.5$, and $\mu = 1$.

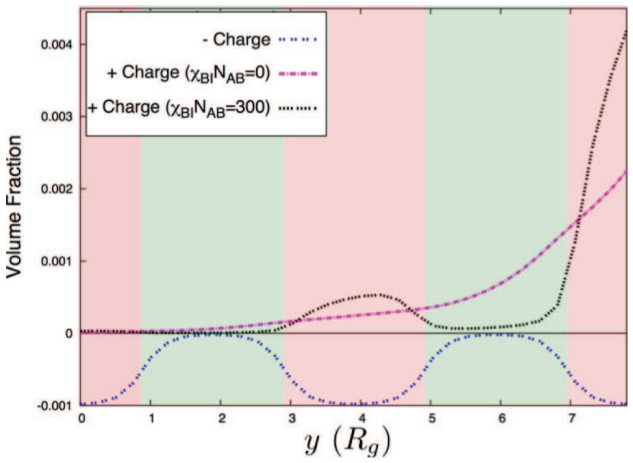


FIG. 9. One dimensional charge distribution for the charged AB system with $P_A = 0.001$, $\chi_{AB}N_{AB} = 20$, $\kappa_A = 6.0$, and $\kappa_B = 2.5$ with $\chi_{BI} = 0$ and $\chi_{BI} = 300$. The positive and negative electrodes are at $y = 0$ and $y = 8R_g$, respectively. The AB polymer distribution is shown as red/green shades, respectively, where in this case, A species are attracted by the substrates.

the addition of free ions. In the present scenario, the charged A species partially wet the top and bottom surfaces in the parallel configuration, which in the presence of an applied external voltage would result in a charge separation of the order of film thickness $L$. This is comparable to the magnitude of charge separation in the perpendicular phase. In fact, in a charged system the parallel configuration is more favorable since both positive and negative charges coat the entire top and bottom plates, while this is only possible to a lesser extent in the perpendicular phase. For this reason, an increase in $P_A$ stabilizes the parallel configuration and thus increases the critical voltage $\Delta V_c$.

We further explore this idea by considering the effect of charge confinement on the critical voltage. As before, we confine the ions by introducing a repulsive interaction between the positive ions and B polymer. The effect of this confinement is shown in Figure 9. An increase in $\chi_{BI}N_{AB}$ results in a greater aggregation of positive ions at the negative electrode and hence a greater separation of charge thereby stabilizing the phase. Again the effect of the repulsive interaction on the free energy

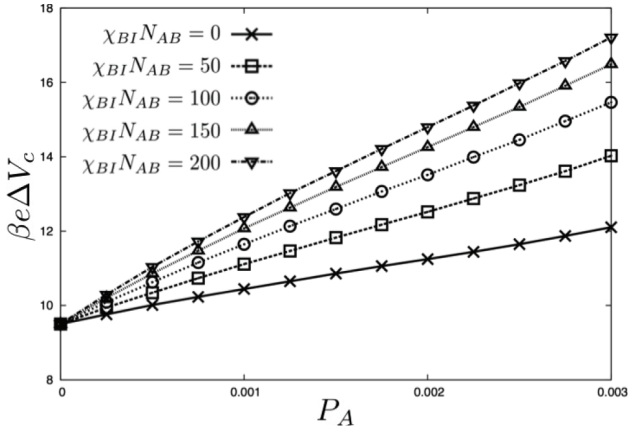


FIG. 10. The critical voltage $\Delta V_c$ plotted as a function of the degree of ionization $P_A$ for a system with $\chi_{AB}N_{AB} = 20$, $\kappa_A = 6.0$, $\kappa_B = 2.5$, and $\mu = 1$.

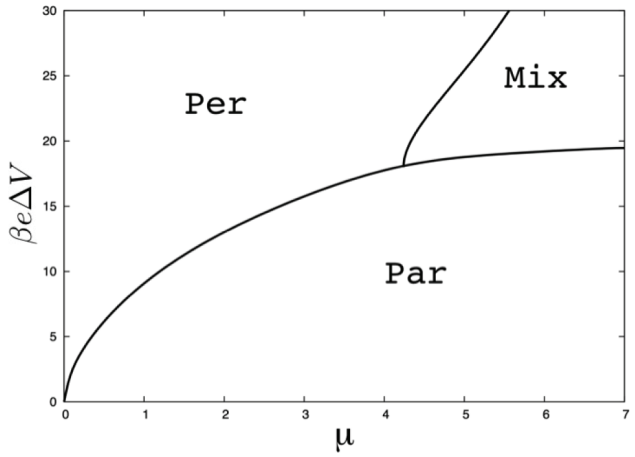


FIG. 11. Phase diagram for the neutral AB system with $P_A = 0$, $\chi_{AB}N_{AB} = 20$, $\chi_{BI}N_{AB} = 0$, $\kappa_A = 6.0$, and $\kappa_B = 2.5$ in the $\Delta V$-$\mu$ plane. The Per, Par, and Mix phases correspond to the perpendicular, parallel, and mixed phases, respectively.

is proportional to the ensemble average of the overlap of ions and B monomers. In the parallel orientation in which the ions are attracted to one plate which is covered by A monomers, the overlap is small so that the free energy is not increased significantly. The overlap is clearly larger in the perpendicular orientation so the free energy of this phase does increase significantly with the imposition of this interaction. Hence, the free energy advantage of the parallel phase increases with the confinement of the ions to the A blocks. Figure 10 shows the critical voltage $\Delta V_c$ as a function of the degree of ionization $P_A$ for various $\chi_{BI}N_{AB}$ values.

We now consider the effect of surface interaction on the voltage required to reorient the lamellae domains from the parallel to the perpendicular orientation. As before, we first consider the phase behavior of neutral AB diblock thin films and then extend our study to the case with charge. Figure 11 presents the phase diagram for the neutral AB system ($P_A = 0$) for a system with $\chi_{AB}N_{AB} = 20$, $\chi_{BI}N_{AB} = 0$, $\kappa_A = 6.0$, and $\kappa_B = 2.5$ in the $\beta e\Delta V$-$\mu$ plane. The phase behavior seen here is similar to that observed in the case in which the neutral

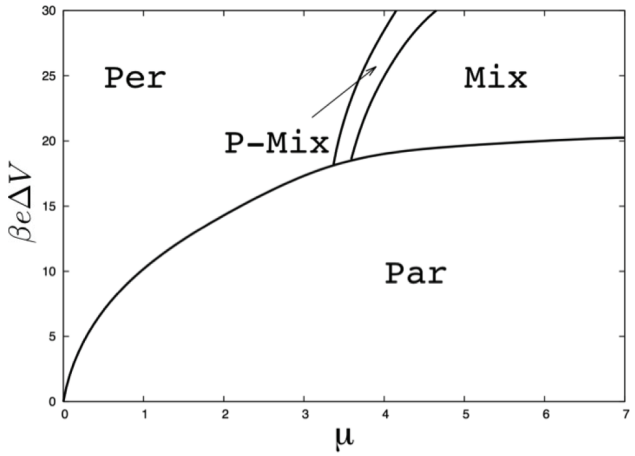


FIG. 12. Phase diagram for the charged AB system with $P_A = 0.003$, $\chi_{AB}N_{AB} = 20$, $\chi_{BI}N_{AB} = 0$, $\kappa_A = 6.0$, and $\kappa_B = 2.5$ in the $\beta e\Delta V$-$\mu$ plane. The Per, Par, Mix, and P-Mix phases correspond to the perpendicular, parallel, mixed, and partially mixed phases, respectively.

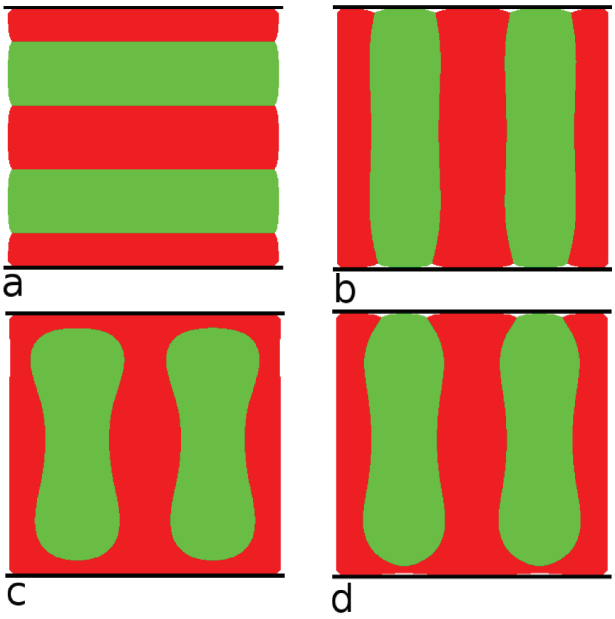


FIG. 13. Density profiles for the (a) parallel, (b) perpendicular, (c) mixed, and (d) partially mixed phases. Here, B species are colored green and A species are colored red. The top/bottom electrodes are negatively/positively charged.

B species was attracted to the substrates, Figure 5. When the applied external voltage is small, the parallel configuration has the lowest free energy. As we increase $\Delta V$, depending on the strength of the surface interaction $\mu$, two scenarios are possible. When the surface interaction is weak, we observe a phase transition from the parallel to the perpendicular phase. When the surface interaction is strong, the phase transition is between the parallel and the mixed phases.

We now turn to the phase behavior of the charged AB diblock copolymer thin films. Figure 12 presents the phase behavior of the charged AB system with $P_A = 0.003$, $\chi_{AB}N_{AB} = 20$, $\chi_{BI}N_{AB} = 0$, $\kappa_A = 6.0$, and $\kappa_B = 2.5$ in the $\Delta V$-$\mu$ plane. The phase behavior seen here is similar to that given in Figure 7, in which the addition of free ions results in the formation of a new partially mixed phase. The density profiles for the parallel, perpendicular, mixed, and partially mixed phases are presented in Figure 13. As before, the addition of charge breaks the symmetry in the effective interaction between the negatively charged A polymers and the positive/negative electrodes. In this scenario, there is a favorable electrostatic and surface interaction between the negatively charge A polymers and positively charged bottom substrate, while there is only the favorable surface interaction between the A species and the negatively charged top surface. At intermediate surface interactions, the A polymers partially wet the bottom surface; however, the extent of such wetting is less at the top plate. At large values of $\mu$, the surface interactions dominate and the A polymers completely cover the top and bottom surfaces resulting in the formation of the mixed phase.

## IV. CONCLUSION

We have examined the effect of the addition of free ions on the magnitude of the external voltage required to reorient a lamellae phase from the parallel configuration to a phase in which domains form perpendicular to the substrates. It was originally suggested by Tsori *et al.*[22,23] that such an addition would reduce the critical voltage $\Delta V_c$. A toy model,[14] which consisted of rigid dielectric media, not block copolymers, indicated that this could be the case provided that certain conditions were met. In particular, Putzel *et al.* suggested that adding charge to a system in which the charged domains are attracted to the surfaces could in fact increase the critical voltage.[14]

In our study, we have examined the behavior of a dielectric material which consists of block copolymers. We have considered two different scenarios, one in which the neutral B blocks are favored by the top and bottom surfaces and the other where the charged A blocks are favored. In both cases, we have examined the effect of adding charge on the critical voltage required to reorient the lamellae from the parallel to the perpendicular morphology. We have also examined the phase behavior of the system as a function of voltage and surface interactions for both neutral and charged films.

In the first case, in which the neutral B polymers were attracted to the surfaces we found that adding charge significantly lowered the critical voltage required to reorient the lamellae from the parallel to the perpendicular orientation. We argued that the decrease in the critical voltage is due to the difference in the magnitude of charge separation in the parallel and perpendicular orientations. We further examined the effect of charge separation on the critical voltage by confining the positive counter ions to the charged A domains. In the confined case in which the difference in magnitude of charge separation between the parallel and perpendicular phase was increased, we found that adding charge would result in much greater reduction in the critical voltage. These results are in accord with experiment.[25,26]

We then considered a scenario in which the charged A polymers were attracted to the substrate surfaces. In this case, adding charge further stabilized the parallel phase and thus resulted in an increase in the critical voltage. We argued that in this scenario, there is no difference in the magnitude of charge separation between the parallel and perpendicular phases. However, in the parallel phase, both the negative and positive ions could coat the entire top and bottom plates, while this coverage is only partial in the perpendicular phase. When the positive counter ions are confined to the A domains, we found that an increase in their density results in an increase in the critical voltage. This interesting behavior should be amenable to experimental verification.

## ACKNOWLEDGMENTS

M.S. would like to thank David Andelman for seminal conversations. This work was supported by the Natural Sciences and Engineering Research Council (NSERC) of Canada, the U.S.-Israel Binational Science Foundation (BSF) under Grant No. 2012060, and the National Science Foundation under Grant No. DMR-1203282. The computation was made possible by the facilities of the Shared Hierarchical Academic Research Computing Network (SHARCNET).

## APPENDIX: THEORETICAL FRAMEWORK

We begin with partition function Eq. (2.5),

$$Z = \Big(\frac{1}{\lambda_I^{3n_I} n_I! \lambda^{3n_{AB}} n_{AB}!}\Big) \times \Big[\int \prod_{i=1}^{n_{AB}} D[\mathbf{R}_i^{AB}(s)] P_{AB}[\mathbf{R}_i^{AB}(s)]\Big] \times \Big[\int \prod_{i=1}^{n_I} d\mathbf{r}_i^I\Big] \exp\Big(-\beta H[\hat{\Phi}_A, \hat{\Phi}_B, \hat{\Phi}_I]\Big) \times \delta\Big(\hat{\Phi}_A(\mathbf{r}) + \hat{\Phi}_B(\mathbf{r}) - 1\Big), \tag{A1}$$

where

$$H[\hat{\Phi}_A, \hat{\Phi}_B, \hat{\Phi}_I] = U[\hat{\Phi}_I, \hat{\Phi}_A] + k_B T \rho_0 \times \int d\mathbf{r}[\chi_{AB}\hat{\Phi}_A(\mathbf{r})\hat{\Phi}_B(\mathbf{r}) + \chi_{BI}\hat{\Phi}_B(\mathbf{r})\hat{\Phi}_I(\mathbf{r})] - k_B T \rho_0 \int d\mathbf{r}\, h(\mathbf{r})[\hat{\Phi}_A(\mathbf{r}) - \hat{\Phi}_B(\mathbf{r})] \tag{A2}$$

and

$$U[\hat{\Phi}_I, \hat{\Phi}_A] = -\frac{1}{2}\int \epsilon(\mathbf{r})[\nabla V(\mathbf{r})]^2 d\mathbf{r} + \rho_0 P_A f \times \int eV(\mathbf{r})[\hat{\Phi}_I(\mathbf{r}) - \frac{\hat{\Phi}_A(\mathbf{r})}{f}] d\mathbf{r}. \tag{A3}$$

The electrostatic potential is itself a functional of $\hat{\Phi}_A$ and $\hat{\Phi}_I$ as it is a solution of the Maxwell equation

$$\nabla \cdot [\epsilon(\mathbf{r})\nabla V(\mathbf{r})] = -eP_A f \rho_0 \big[\hat{\Phi}_I(\mathbf{r}) - \hat{\Phi}_A(\mathbf{r})/f\big], \tag{A4}$$

with a boundary condition of the specified voltages on the plates. Given that Maxwell's equations for the electric and displacement fields have been used to derive the electrostatic energy, Eq. (A3), it may not be too surprising that this energy is an extremum with respect to the potential $V$, i.e., $\delta U[V]/\delta V = 0$ leads to Eq. (A4). We now derive the SCFT approximation to the free energy. To make the self-consistent field approximation transparent, it is convenient to rewrite the partition function by introducing auxiliary fields $W_A(\mathbf{r})$ and $\Phi_A(\mathbf{r})$, and $W_B(\mathbf{r})$ and $\Phi_B(\mathbf{r})$ via the identities

$$\int DW_A D\Phi_A \exp\left\{\frac{n_{AB}}{\Omega}\int d\mathbf{r}\, iW_A(\mathbf{r})\big[\Phi_A(\mathbf{r}) - \hat{\Phi}_A(\mathbf{r})\big]\right\} = 1, \tag{A5}$$

$$\int DW_B D\Phi_B \exp\left\{\frac{n_{AB}}{\Omega}\int d\mathbf{r}\, iW_B(\mathbf{r})\big[\Phi_B(\mathbf{r}) - \hat{\Phi}_B(\mathbf{r})\big]\right\} = 1. \tag{A6}$$

Similarly, we utilize

$$\int D\Phi_I DW_I \exp\left\{\rho_I \int d\mathbf{r}\, iW_I(\mathbf{r})[\Phi_I(\mathbf{r}) - \hat{\Phi}_I(\mathbf{r})]\right\} = 1. \tag{A7}$$

With the introduction of these fields, we rewrite the incompressibility constraint in the form

$$\delta\Big(\hat{\Phi}_A(\mathbf{r}) + \hat{\Phi}_B(\mathbf{r}) - 1\Big) = \int D\xi \exp\left\{\frac{n_{AB}}{\Omega}\int d\mathbf{r}\, i\xi(\mathbf{r})\left[\Phi_A(\mathbf{r}) + \Phi_B(\mathbf{r}) - 1\right]\right\}. \tag{A8}$$

Utilizing the above identities, we can rewrite the partition function in the form

$$Z = \int DW_A D\Phi_A DW_B D\Phi_B DW_I D\Phi_I D\xi DV \exp\left\{-\beta\mathcal{F}[W_A, \Phi_A, W_B, \Phi_B, W_I, \Phi_I, \xi]\right\}, \tag{A9}$$

where

$$\beta\mathcal{F} = -n_I \ln(Q_I[iW_I]/n_I) - n_{AB}\ln(Q_{AB}[iW_A, iW_B]/n_{AB}) - fP_A\rho_0\int dr\, iW_I(\mathbf{r})\Phi_I(\mathbf{r}) - \beta\rho_0\int d\mathbf{r}\frac{1}{2\rho_0}\epsilon(\mathbf{r})(\nabla V(\mathbf{r}))^2 + \beta f P_A \rho_0 \int d\mathbf{r}\, V(\mathbf{r})e[\Phi_I(\mathbf{r}) - \Phi_A(\mathbf{r})/f] + \rho_0\int d\mathbf{r}[\chi_{AB}\Phi_A(\mathbf{r})\Phi_B(\mathbf{r}) + \chi_{BI}\Phi_B(\mathbf{r})\Phi_I(\mathbf{r})] - \rho_0\int d\mathbf{r}h(\mathbf{r})[\Phi_A(\mathbf{r}) - \Phi_B(\mathbf{r})] - \frac{n_{AB}}{\Omega}\int d\mathbf{r}\,[iW_A(\mathbf{r})\Phi_A(\mathbf{r}) + iW_B(\mathbf{r})\Phi_B(\mathbf{r}) + i\xi(\mathbf{r})(\Phi_A(\mathbf{r}) + \Phi_B(\mathbf{r}) - 1)]. \tag{A10}$$

In the above equation, $Q_{AB}[iW_A, iW_B]$ is the partition function of a single polymer chain in the fields $iW_A$ and $iW_B$, and $Q_I[iW_I]$ is the partition function of a single ion in the field $iW_I$,

$$Q_I[iW_I] \equiv \frac{\Omega}{\lambda_I^3}\int d\mathbf{r}\frac{\exp\{-iW_I(\mathbf{r})\}}{\Omega}. \tag{A11}$$

In addition, the charge neutrality condition, $\rho_I = P_A f \rho_0$, has been used. The electrostatic potential, $V(\mathbf{r})$, is obtained from the Maxwell equation

$$\nabla \cdot [\epsilon(\mathbf{r})\nabla V(\mathbf{r})] = -eP_A f \rho_0[\Phi_I(\mathbf{r}) - \Phi_A(\mathbf{r})/f], \tag{A12}$$

which is completely equivalent to Eq. (A4) because of the identities Eqs. (A5) and (A7). Thus, at this point, the electrostatic potential varies with the distinct configurations of charges.

The above transformations are exact, but the integrals cannot be carried out in general. Self-consistent field theory results from extremizing the functional $\beta\mathcal{F}$ with respect to the seven functions on which it depends. Extremizing with respect to $W_A$ and $W_B$, we obtain

$$\Phi_A(\mathbf{r}) = \langle\hat{\Phi}_A(\mathbf{r})\rangle, \tag{A13}$$

$$\Phi_B(\mathbf{r}) = \langle\hat{\Phi}_B(\mathbf{r})\rangle, \tag{A14}$$

where $\langle\hat{\Phi}_A(\mathbf{r})\rangle$ is the average of $\hat{\Phi}_A(\mathbf{r})$ in the ensemble of a single polymer in the fields $iW_A$ and $iW_B$, and similarly for $\langle\hat{\Phi}_B(\mathbf{r})\rangle$. Variation with respect to $W_I$ yields

$$\Phi_I(\mathbf{r}) = \frac{\exp[-iW_I(\mathbf{r})]}{(1/\Omega)\int \exp[-iW_I(\mathbf{r})]d\,\mathbf{r}}. \tag{A15}$$

Extremizing with respect to $\Phi_A, \Phi_B$, and $\Phi_I$ and utilizing the fact that $\mathcal{F}$, like the electrostatic energy $U$, is an extremum with respect to variations in the potential $V$ ensuring that $\{\delta\mathcal{F}/\delta V[\Phi_A, \Phi_I]\}\{\delta V/\delta\Phi_\alpha\} = 0, \alpha = A, B, I$, we obtain

$$\frac{iW_a(\mathbf{r})}{N_{AB}} = \chi_{AB}\Phi_B(\mathbf{r}) - \frac{\kappa_A}{8\pi\ell\rho_0}[\nabla\beta eV(\mathbf{r})]^2 - P_A\beta eV(\mathbf{r}) - h(\mathbf{r}) - i\frac{\xi(\mathbf{r})}{N_{AB}}, \tag{A16}$$

$$\frac{iW_B(\mathbf{r})}{N_{AB}} = \chi_{AB}\Phi_A(\mathbf{r}) + \chi_{BI}\Phi_I(\mathbf{r}) - \frac{\kappa_B}{8\pi\ell\rho_0}[\nabla\beta eV(\mathbf{r})]^2 + h(\mathbf{r}) - i\frac{\xi(\mathbf{r})}{N_{AB}}, \tag{A17}$$

$$iW_I(\mathbf{r}) = \beta eV(\mathbf{r}). \tag{A18}$$

Finally, variation with respect to $\xi$ produces

$$\Phi_A(\mathbf{r}) + \Phi_B(\mathbf{r}) = 1. \tag{A19}$$

The value of the electrostatic potential averaged over all configurations of the charges, $\langle V[\hat{\Phi}_A, \hat{\Phi}_I]\rangle$, is approximated in self-consistent field theory by the value of the same functional evaluated at the ensemble average values of the charge densities $V[\langle\hat{\Phi}_A\rangle, \langle\hat{\Phi}_I\rangle]$.

Similarly, the free energy in the self-consistent field approximation, $F_{scft}$, is the value of the functional $\mathcal{F}$ above evaluated with the functions that satisfy the self-consistent equations

$$\frac{\beta F_{scft}}{n_{AB}} = -P_A f N_{AB}\ln(Q_I/n_I) - \ln(Q_{AB}/n_{AB}) - \frac{1}{\Omega}\int d\mathbf{r}\chi_{AB}N_{AB}\Phi_A(\mathbf{r})\Phi_B(\mathbf{r}) \tag{A20}$$

$$- \frac{1}{\Omega}\int d\mathbf{r} i\xi(\mathbf{r}). \tag{A21}$$

We can eliminate the explicit appearance of the partition function $Q_I$ by the use of Eqs. (A18) and (A15)

$$-\ln Q_I/n_I = \beta eV(\mathbf{r}) + \ln\left(\frac{\Phi_I(\mathbf{r})\lambda_I^3}{\Omega}\right) + \ln n_I. \tag{A22}$$

We multiply the above by $n_I\Phi_I(\mathbf{r})$ and integrate over the volume to obtain the free energy of the ions, $F_I$,

$$F_I = -k_BTn_I\ln Q_I/n_I = \rho_I\int d\mathbf{r}\Phi_I(\mathbf{r})[eV(\mathbf{r}) + k_BT\ln\Phi_I(\mathbf{r})] + n_Ik_BT\ln\left(\frac{n_I\lambda_I^3}{\Omega}\right). \tag{A23}$$

We substitute this into Eq. (A20) and again use charge neutrality to obtain

$$\frac{\beta F_{scft}}{n_{AB}} = -\ln(Q_{AB}/n_{AB}) - \frac{1}{\Omega}\int d\mathbf{r}\chi_{AB}N_{AB}\Phi_A(\mathbf{r})\Phi_B(\mathbf{r}) \tag{A24}$$

$$+ P_A f N_{AB}\int d\mathbf{r}\,[\beta eV(\mathbf{r})\Phi_I(\mathbf{r}) + \Phi_I(\mathbf{r})\ln\Phi_I(\mathbf{r})] + n_I\ln\left(\frac{n_I\lambda_I^3}{\Omega}\right), \tag{A25}$$

where we have set to zero the integral over the volume of $\xi(\mathbf{r})$. This is the expression we seek for the free energy of the system within self-consistent field theory. We shall ignore the last term as it is a constant in the canonical ensemble.


[1]T. Thurn-Albrecht, J. Schotter, G. Kästle, N. Emley, T. Shibauchi, L. Krusin-Elbaum, K. Guarini, C. Black, M. Tuominen, and T. Russell, Science **290**, 2126 (2000).
[2]M. Park, C. Harrison, P. M. Chaikin, R. A. Register, and D. H. Adamson, Science **276**, 1401 (1997).
[3]C. Leidel, C. W. Pester, M. Ruppel, V. S. Urban, and A. Böker, Macromol. Chem. Phys. **213**, 259 (2012).
[4]S. O. Kim, H. H. Solak, M. P. Stoykovich, N. J. Ferrier, J. J. de Pablo, and P. F. Nealey, Nature **424**, 411 (2003).
[5]M. P. Stoykovich, M. Müller, S. O. Kim, H. H. Solak, E. W. Edwards, J. J. De Pablo, and P. F. Nealey, Science **308**, 1442 (2005).
[6]S. O. Kim, B. H. Kim, D. Meng, D. O. Shin, C. M. Koo, H. H. Solak, and Q. Wang, Adv. Mater. **19**, 3271 (2007).
[7]D. O. Shin, B. H. Kim, J.-H. Kang, S.-J. Jeong, S. H. Park, Y.-H. Lee, and S. O. Kim, Macromolecules **42**, 1189 (2009).
[8]S. Park, D. H. Lee, J. Xu, B. Kim, S. W. Hong, U. Jeong, T. Xu, and T. P. Russell, Science **323**, 1030 (2009).
[9]D. Sundrani, S. Darling, and S. Sibener, Nano Lett. **4**, 273 (2004).
[10]R. A. Segalman, H. Yokoyama, and E. J. Kramer, Adv. Mater. **13**, 1152 (2001).
[11]T. Morkved, M. Lu, A. Urbas, E. Ehrichs, H. Jaeger, P. Mansky, and T. Russell, Science **273**, 931 (1996).
[12]K. Amundson, E. Helfand, X. Quan, and S. D. Smith, Macromolecules **26**, 2698 (1993).
[13]Y. Tsori and D. Andelman, Macromolecules **35**, 5161 (2002).
[14]G. G. Putzel, D. Andelman, Y. Tsori, and M. Schick, J. Chem. Phys. **132**, 164903 (2010).
[15]C.-Y. Lin, M. Schick, and D. Andelman, Macromolecules **38**, 5766 (2005).
[16]C.-Y. Lin and M. Schick, J. Chem. Phys. **125**, 034902 (2006).
[17]Q. Tong and S. Sibener, J. Phys. Chem. C **118**, 13752 (2014).
[18]M. Ruppel, C. W. Pester, K. M. Langner, G. J. Sevink, H. G. Schoberth, K. Schmidt, V. S. Urban, J. W. Mays, and A. Boker, ACS Nano **7**, 3854 (2013).
[19]P. Goldberg-Oppenheimer, D. Kabra, S. Vignolini, S. Huttner, M. Sommer, K. Neumann, M. Thelakkat, and U. Steiner, Chem. Mater. **25**, 1063 (2013).
[20]S. Elhadj, J. Woody, V. Niu, and R. Saraf, Appl. Phys. Lett. **82**, 871 (2003).
[21]T. Xu, A. Zvelindovsky, G. Sevink, K. Lyakhova, H. Jinnai, and T. Russell, Macromolecules **38**, 10788 (2005).
[22]Y. Tsori, F. Tournilhac, and L. Leibler, Macromolecules **36**, 5873 (2003).
[23]Y. Tsori, F. Tournilhac, D. Andelman, and L. Leibler, Phys. Rev. Lett. **90**, 145504 (2003).
[24]M. Matsen, Macromolecules **39**, 5512 (2006).
[25]J.-Y. Wang, T. Xu, J. M. Leiston-Belanger, S. Gupta, and T. P. Russell, Phys. Rev. Lett. **96**, 128301 (2006).

[26]P. Kohn, K. Schröter, and T. Thurn-Albrecht, Phys. Rev. Lett. **102**, 216101 (2009).
[27]J. Marko and Y. Rabin, Macromolecules **25**, 1503 (1992).
[28]R. Kumar and M. Muthukumar, J. Chem. Phys. **126**, 214902 (2007).
[29]I. Nakamura, N. Balsara, and Z.-G. Wang, Phys. Rev. Lett. **107**, 198301 (2011).
[30]S. Yang, A. Vishnyakov, and A. Neiman, J. Chem. Phys. **134**, 054104 (2011).
[31]C. Sing, J. W. Zwanikken, and M. O. de la Cruz, Nat. Mater. **13**, 694 (2014).
[32]T. Xu, J. T. Goldbach, J. Leiston-Belanger, and T. P. Russell, Colloid Polym. Sci. **282**, 927 (2004).
[33]M. Matsen, in *Soft Matter Vol 1: Polymer Melts and Mixtures*, edited by G. Gompper and M. Schick (Wiley-VCH, Weinheim, 2006).
[34]F. Schmid, J. Phys.: Condens. Matter **10**, 8105 (1998).
[35]A.-C. Shi and J. Noolandi, Macromol. Theory Simul. **8**, 214 (1999).
[36]G. H. Fredrickson, V. Ganesan, and F. Drolet, Macromolecules **35**, 16 (2002).
[37]G. H. Fredrickson, *The Equilibrium Theory of Inhomogeneous Polymers* (Clarendon, 2006).
[38]M. Turner, Phys. Rev. Lett. **69**, 1788 (1992).
[39]M. Matsen, J. Chem. Phys. **106**, 7781 (1997).
[40]R. Messina, C. Holm, and K. Kremer, J. Polym. Sci., Part B: Polym. Phys. **42**, 3557 (2004).